CME LIVE OPEN ACCESS

Journal of
Veterinary Research and Clinical Care

Research Article

ISSN: 3065-9000

Molecular Dynamics Simulation of *Aloe Barbadensis* Anthraquinones Targeting MRSA Peptidoglycan Biosynthesis Enzymes

Loice Naswa Wechuli and Stephen S Barasa*

Department of Chemistry and Biochemistry, University of Eldoret, P.O. Box 1125 30100, Eldoret, Kenya.

Corresponding Author: Stephen S Barasa https://orcid.org/0000-0003-1116-1523, Loice Naswa Wechuli https://orcid.org/0009-0002-6775-0394 Department of Chemistry and Biochemistry, University of Eldoret, Kenya.

Received: 2026 Apr 01 **Accepted:** 2026 May 06 **Published:** 2026 Jun 15

Abstract

Antibiotic resistance is a major threat to world health organisation(WHO). Methicillin resistant staphylococcus aureus(MRSA) one of the dangerous pathogens. Is commonly found on skin surface, congested places and even in blood stream, for decades' gentamycin has been used to inhibit the bacterium biofilm though the number of mortality rates have been increasing up to date. The evolution of drug resistance has led to the use of traditional medicinal plants such as Artemisia annua and aloe barbadense. The respective crude extracts showed inhibition of the bacterium staphylococcus aureus while the combined use of the Artemisia annua and Aloe barbadense crude extracts showed increased synergy. However, no precise phytochemicals have been done to identify the specific drug like compound responsible for the activity against staphylococcus aureus pathogen. This present study identifies the specific drug like compound(s) via Insilco array of study against Methicillin resistant staphylococcus aureus MurB target (MRSA-MurB).

Keywords: Molecular, Peptidoglycan, MRSA, Phytochemicals

1. Introduction

Around the globe *Artemisia annua* and *Aloe barbadense* have been known locally as medicinal plants used traditionally by our forefathers. The two medicinal plants have played a greater role in the drug industry in designing different drugs. *Staphylococcus aureus* on the other side is one of the pathogens of great concern globally due it is known ability to antibiotic resistance [1-3]. Since the year 1978 Gentamicin has been the only drug that is being used upto date as the antibiotic measure of pathogen of *Staphylococcus aureus*. This causes drug abuse and misuse in some cases since at time a patient will be forced to take in more than what it has been described by the specialist thus increasing the rate of body resistance [4-6]. The crude extracts of *Artemisia annua* and *Aloe barbadense* have been used against *Staphylococcus aureus* pathogen for decades and the have shown the antimicrobial activity against the bacterium thus inhibiting biofilm formation [7-9]. However, the combined use of the crude extracts from *Artemisia annua* and *Aloe barbadense* miller showed increased synergy against the *Staphylococcus aureus* [10]. *Aloe barbadense* has only forty six compounds where one of its compounds was tested and shown inhibition against *staphylococcus aureus* [11,12]. This study focuses on identifying drug like compound(s) from the mentioned forty six (46) responsible for the phytochemical activity of *Staphylococcus aureus* using In-silico approach.

2. Materials and Method

2.1. Selection and Preparation of Phytochemicals

The reported bioactive compounds from *A. barbadensis* were identified from the literature and public databases (PubChem, ChemSpider) [13]. A total of 28 compounds were initially considered. Its 3D structures were downloaded as SDF files and converted to PDBQT format using Open Babel and AutoDock Tools [14].

2.2. Selection and Preparation of Protein Targets

Eleven MRSA protein structures were retrieved from the Protein Data Bank (PDB). Table 1 summarizes the targets, their functions, and PDB IDs.

Target	Gene(s)	Function	PDB ID	Reference
Penicillin-binding protein 2a (PBP2a)	*mecA*	Peptidoglycan transpeptidase (β lactam resistance)	1VQQ	Lim & Strynadka (2002)
DNA gyrase (GyrA/GyrB)	*gyrA/gyrB*	DNA supercoiling (type II topoisomerase)	5Z9N	Chan et al. (2019)
Topoisomerase IV (ParC/ParE)	*parC/pare*	Decatenation of replicated chromosomes	3RAF	Laponogov et al. (2010)
Dihydrofolate reductase (DHFR)	*folA*	Tetrahydrofolate synthesis (one carbon metabolism)	3FQ0	Heaslet et al. (2009)
Dihydropteroate synthase (DHPS)	*folP*	Folate biosynthesis	1AD4	Hampele et al. (1997)
MurA	*murA*	First committed step in peptidoglycan synthesis	1UAE	Eschenburg et al. (2002)
MurB	*murB*	Peptidoglycan precursor formation (dehydrogenase)	1MBT	Benson et al. (1996)
FemA / FemB	*femA/femB*	Pentaglycine bridge formation in S. aureus PG	6U6B	Millay et al. (2020)
Sortase A (SrtA)	*srtA*	LPXTG surface protein anchoring (virulence)	1T2W	Suree et al. (2009)
ClpP (caseinolytic protease)	*clpP*	Protein quality control / stress responses	3KTJ	Geiger et al. (2011)
LtaS (lipoteichoic acid synthase)	*ltaS*	Lipoteichoic acid synthesis (cell envelope)	7QMU	Li et al. (2021)

Table 1: MRSA Target Proteins Used in Docking

Protein structures were prepared by removing water molecules and heteroatoms (except co crystallized ligands used for active site identification), adding polar hydrogens, assigning Kollman charges, and performing energy minimization using AutoDock Tools.

2.3. Molecular Docking Procedure

Molecular docking was done using AutoDock Vina . Grid boxes were centered on the active sites of every target, as defined by co crystallized inhibitors or literature reported binding pockets. The grid dimensions were set to 20 × 20 × 20 Å for most targets, with exhaustiveness set to 8–16. Binding affinities (ΔG in kcal/mol) were recorded; less negative values indicate good binding while positive values indicate weak binding/ unfavourable. The docking protocol was then justified by re docking co crystallized ligands and comparing root mean square deviation (RMSD) values (all < 2.0 Å). Visualization of ligand protein interactions was performed using PyMOL (The PyMOL Molecular Graphics System, Version 2.0) and Discovery Studio Visualizer (Dassault Systèmes).

3. Results and Discussion

Twenty eight compounds from *Aloe barbadense's* were selected

Aloe barbadense				
Name	**MolWt**	**LogP**	**HBD**	**HBA**
Chrysophanol	254.241	2.18162	2	4
Aloeresin	394.376	-0.5466	5	9
3,4-Dihydroxybenzoic acid	154.121	0.796	3	3
Aloe emodin	270.24	1.3655	3	5
1,5-Dihydroxy-3-methylanthraquinone	254.241	2.18162	2	4
7-O-Methylaloesin	408.403	-0.2436	4	9
7-O-Methylaloesinol	410.419	-0.4518	5	9

Feroxidin	194.23	1.5084	3	3
Nataloin	411.342	2.69792	0	2
Aloechrysone	272.3	2.4339	2	4
Aloe barbendol	258.273	2.04922	3	4
Aloenin	410.375	-0.4919	5	10
Aloesaponol I	316.309	1.83582	3	6
Aloesaponarin I	312.277	1.96822	2	6
Aloesaponol II	258.273	2.04922	3	4
Aloesaponarin II	254.241	2.18162	2	4
Isoeleutherol	244.246	2.7854	1	4
Aloesaponol IV	288.299	2.19422	3	5
Ziganein-5-methyl ether	268.268	2.48462	1	4
Pluridone	236.292	2.2892	0	4
Luteolin	286.239	2.2824	4	6
Kaempferol	286.239	2.2824	4	6
Quercetin	302.238	1.988	5	7
Oxalic acid	90.034	-0.8444	2	2
Salicylic acid	138.122	1.0904	2	2
Caffeic acid	180.159	1.1956	3	3
p-Coumaric acid	164.16	1.49	2	2
Ferulic acid	194.186	1.4986	2	3

Table 2: Compounds of *Aloe Barbadense* that were Assessed

Table 2 shows the molecular weight of different compounds presents in aloe barbadense. According to Lipinski rule of five (5) ; a compound is drug-like if it has moleculer weight below or equal to 500, HBA<5, HBD<10 and logP<5. With the results above , aloesaponarin-I is a drug like compound.

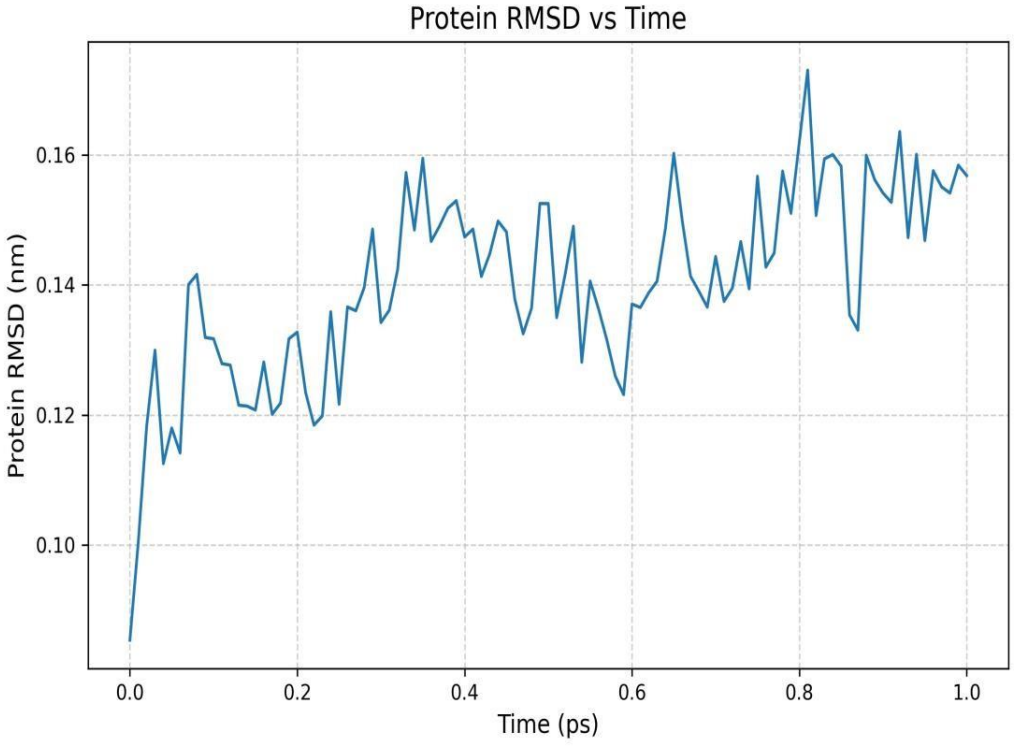

Figure 1: Protein RMSD

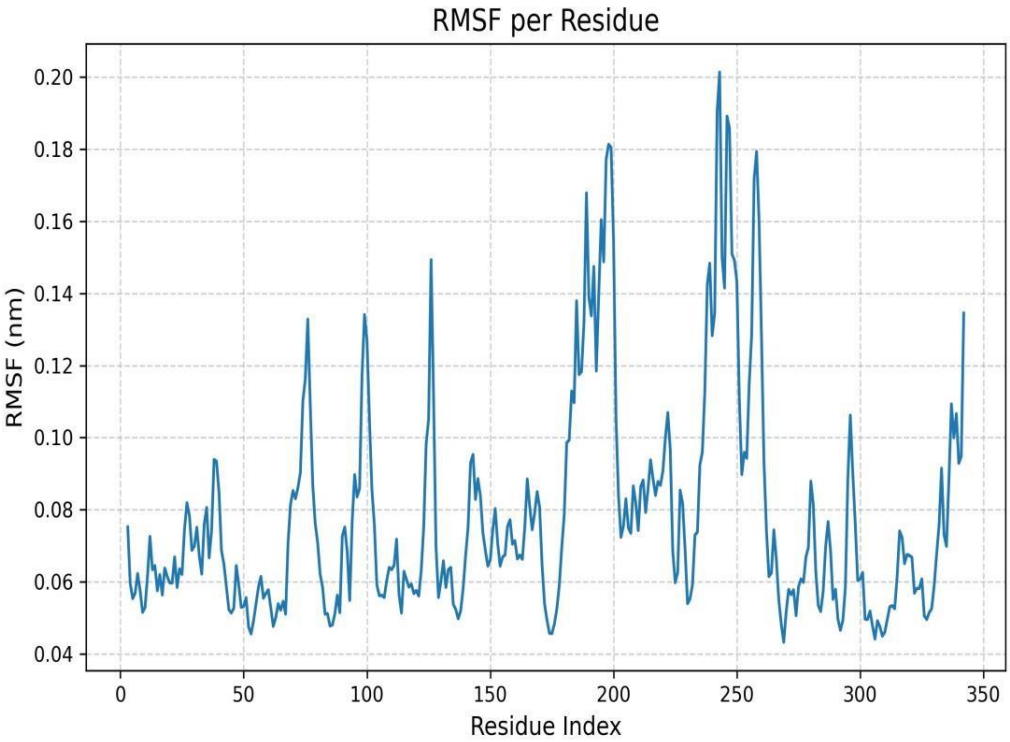

Figure 2: RMSF

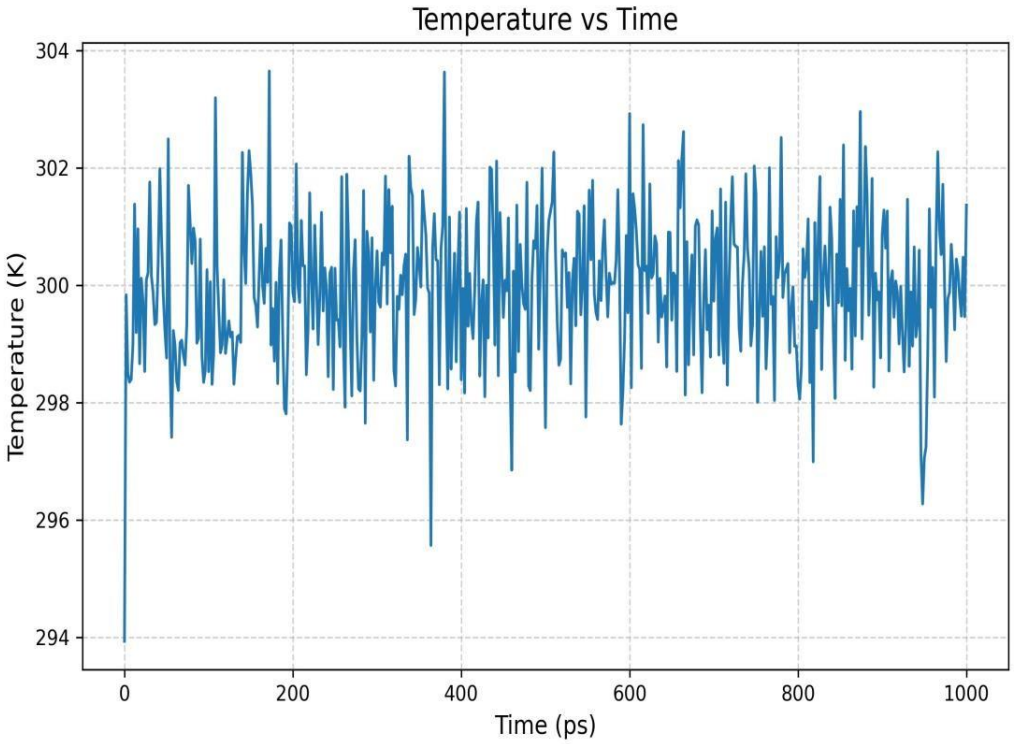

Figure 3: Temperature

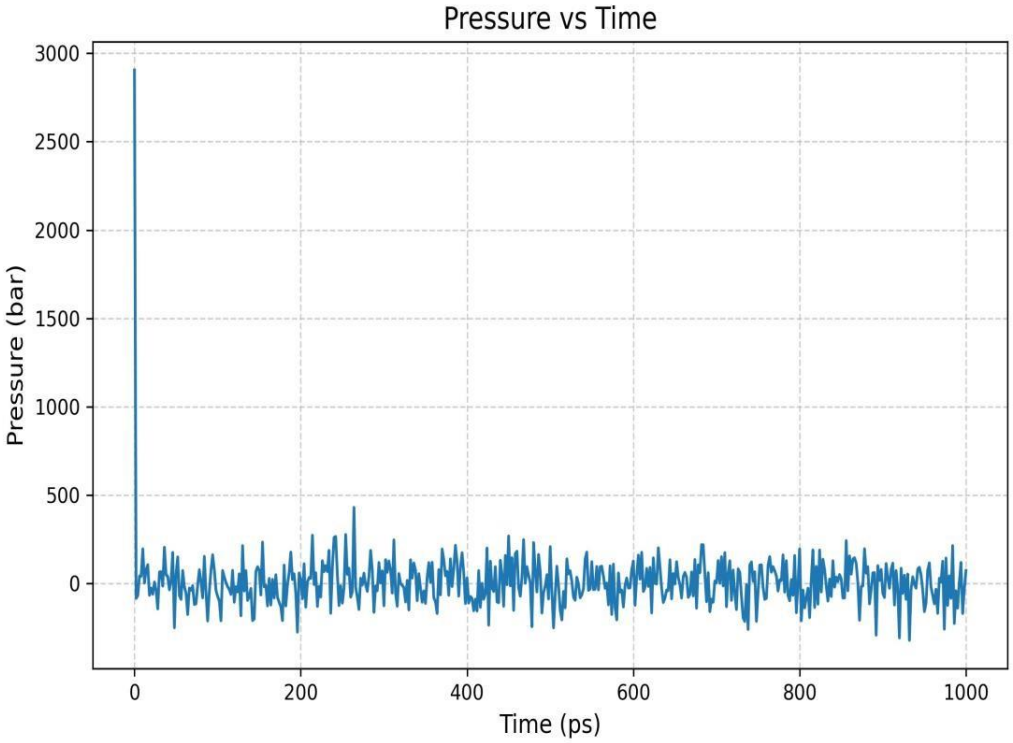

Figure 4: Pressure

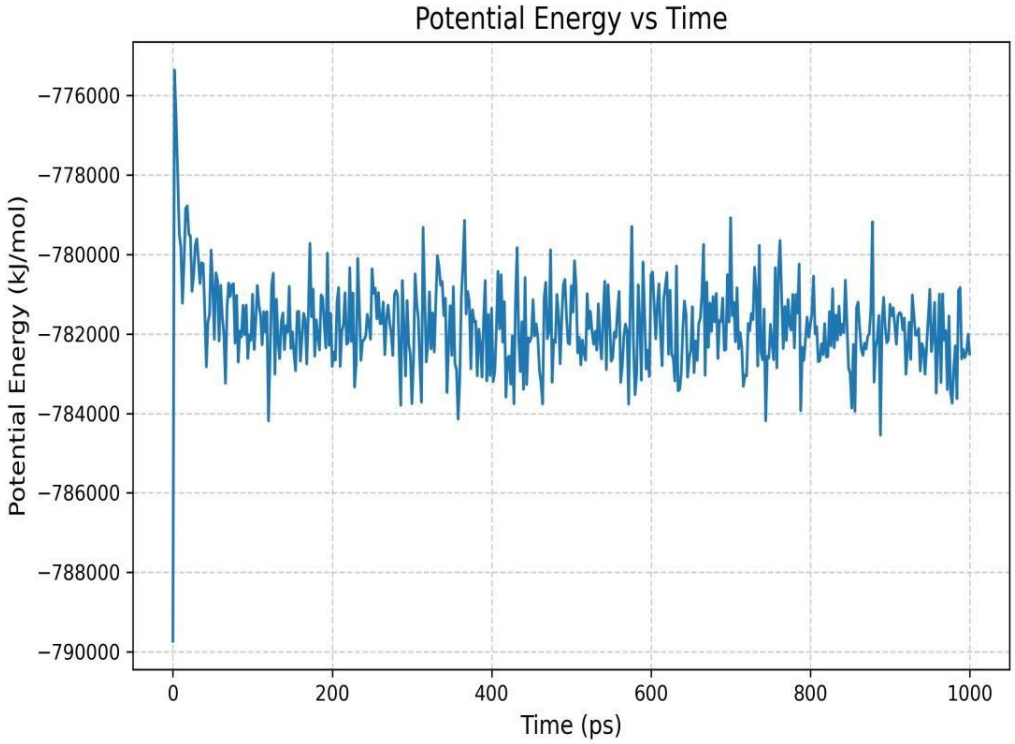

Figure 5: Potential

Citation: Wechuli, L. N., Barasa, S. S. (2026). Molecular Dynamics Simulation of *Aloe Barbadensis* Anthraquinones Targeting MRSA Peptidoglycan Biosynthesis Enzymes. *J Vet Res Clin Care, 3*(1), 1-12.

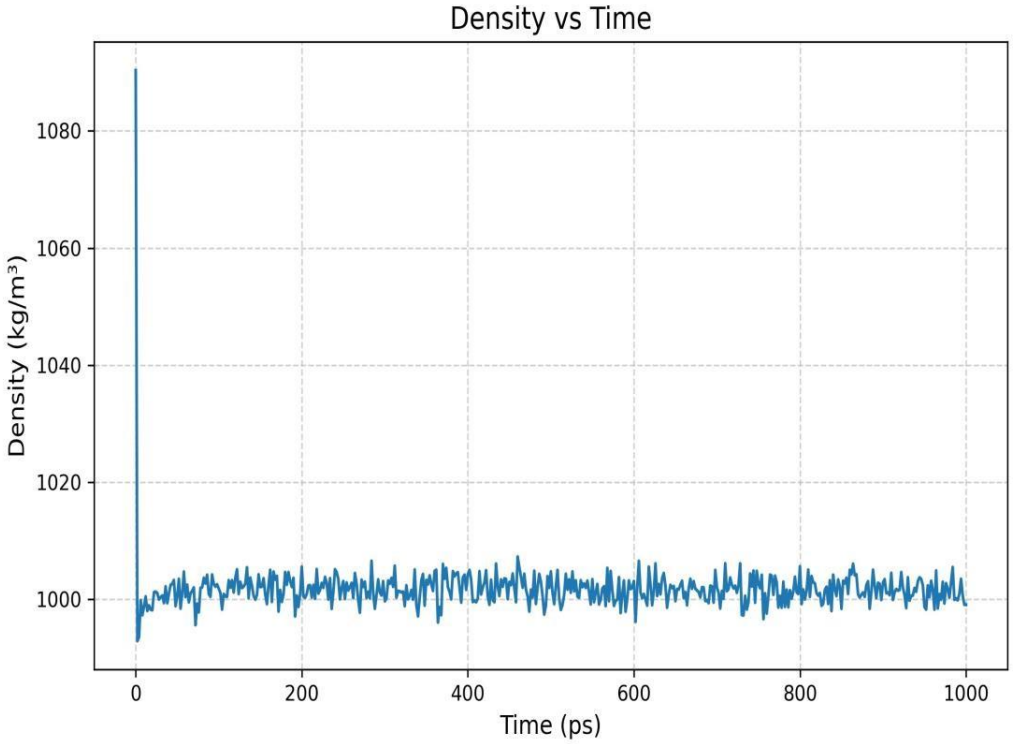

Figure 6: Density

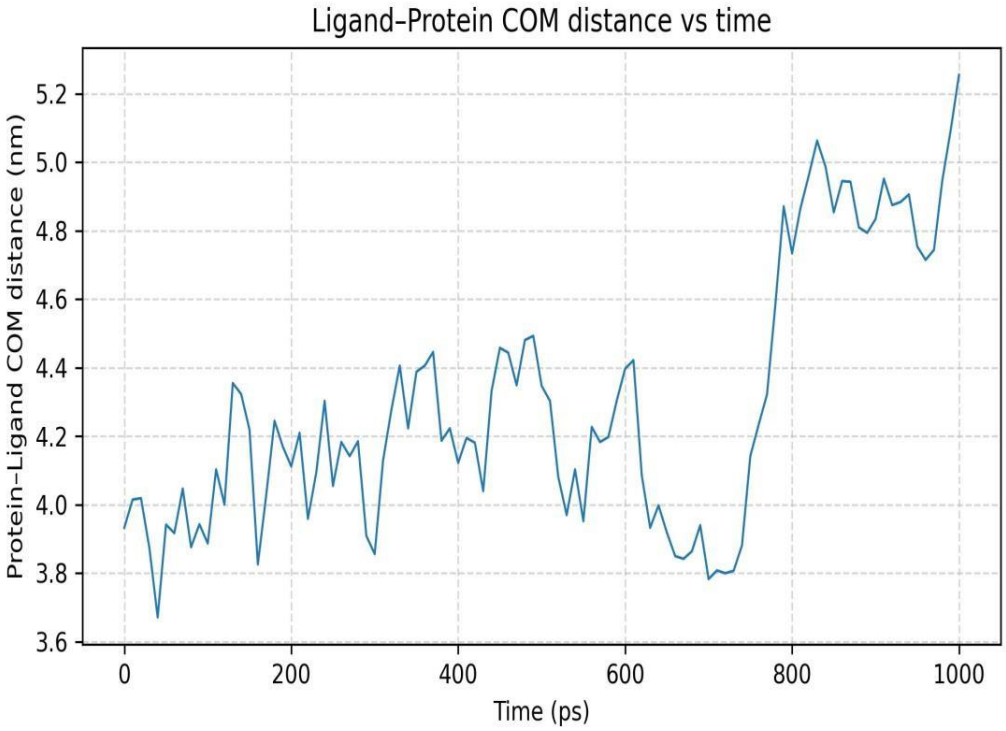

Figure 7: COM Distance

Citation: Wechuli, L. N., Barasa, S. S. (2026). Molecular Dynamics Simulation of *Aloe Barbadensis* Anthraquinones Targeting MRSA Peptidoglycan Biosynthesis Enzymes. *J Vet Res Clin Care, 3*(1), 1-12.

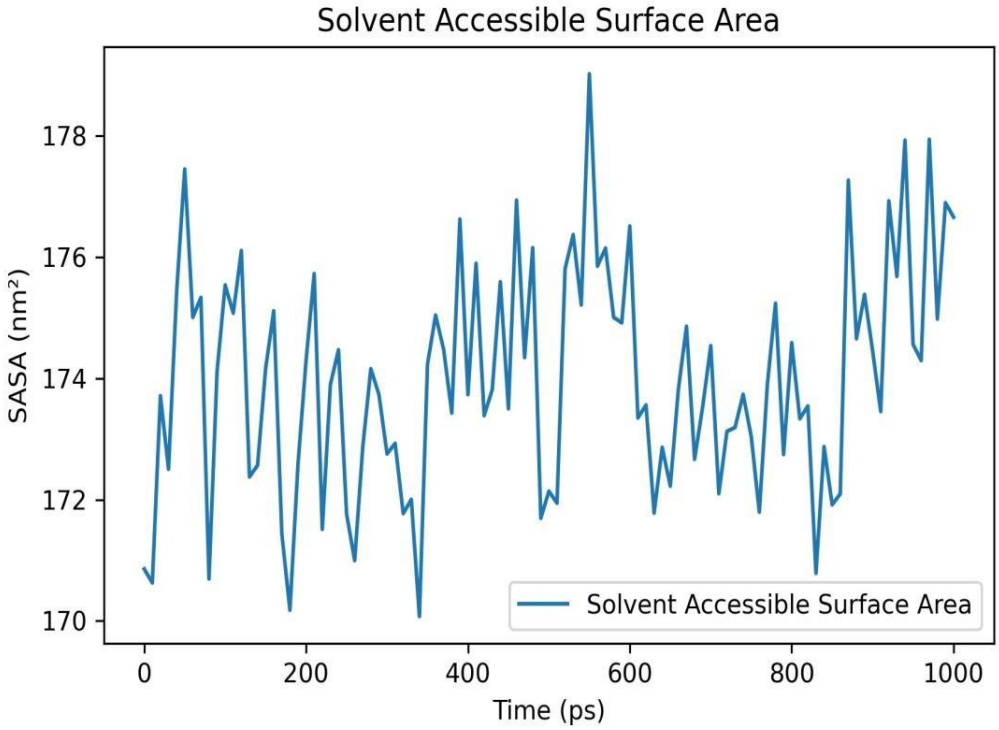

Figure 8: SASA

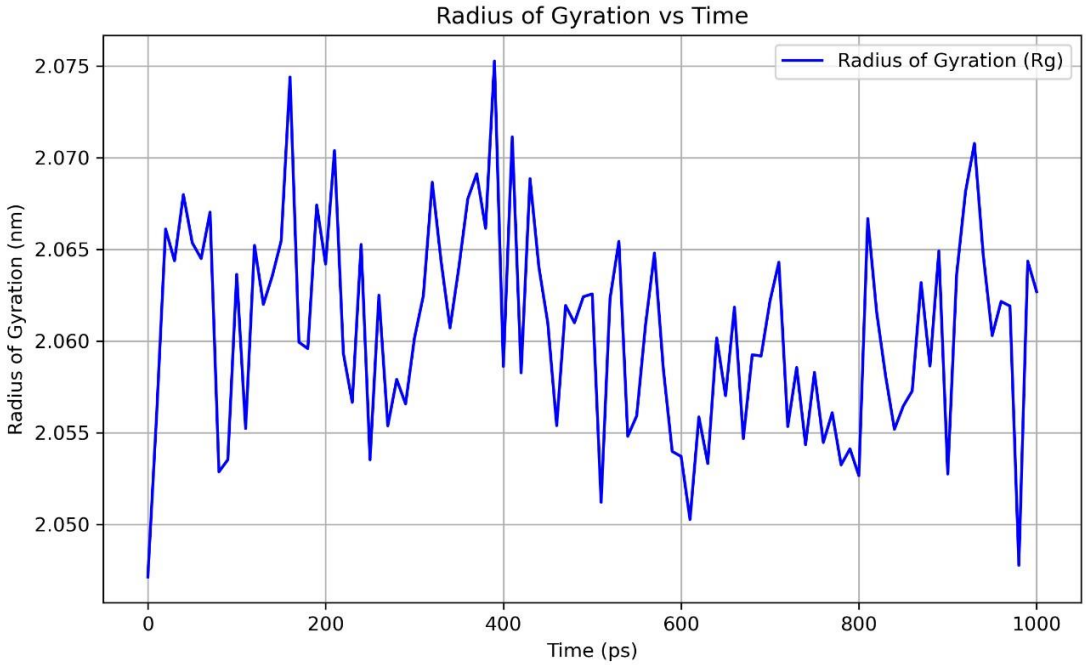

Figure 9: Radius of Gyration

Citation: Wechuli, L. N., Barasa, S. S. (2026). Molecular Dynamics Simulation of *Aloe Barbadensis* Anthraquinones Targeting MRSA Peptidoglycan Biosynthesis Enzymes. *J Vet Res Clin Care, 3*(1), 1-12.

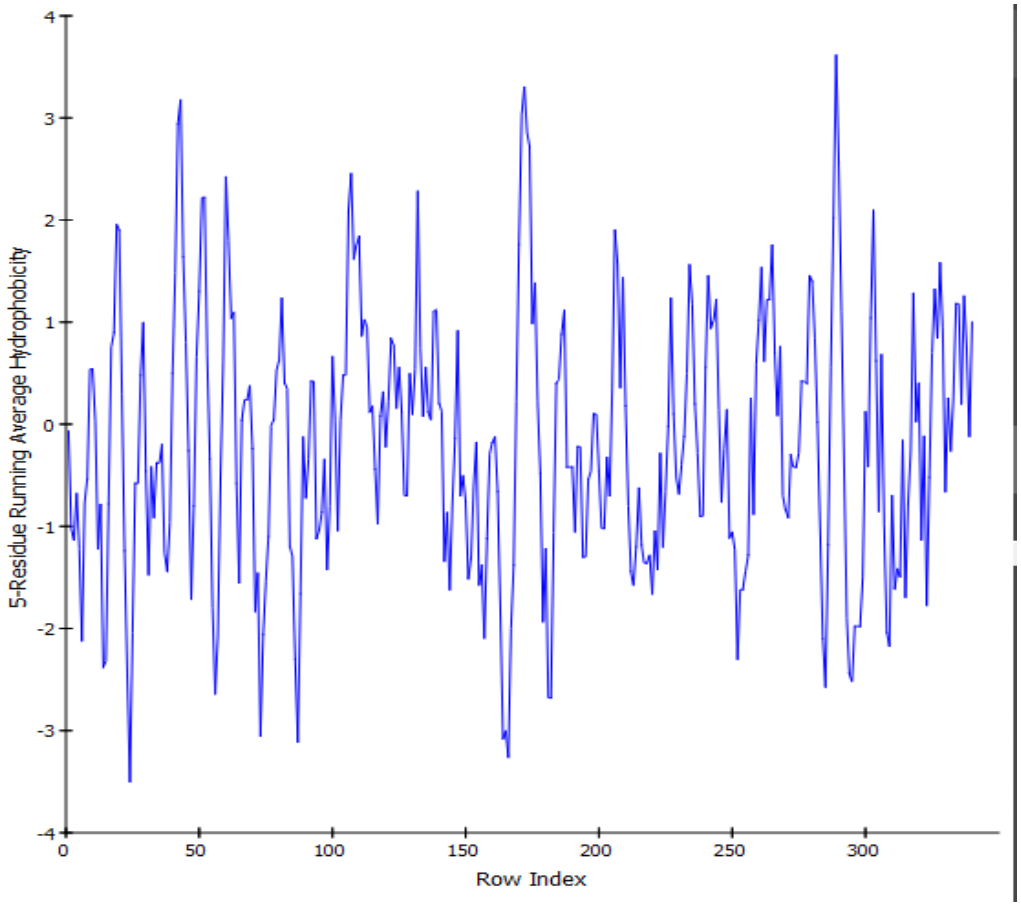

Figure 10: Hydrophobicity Index

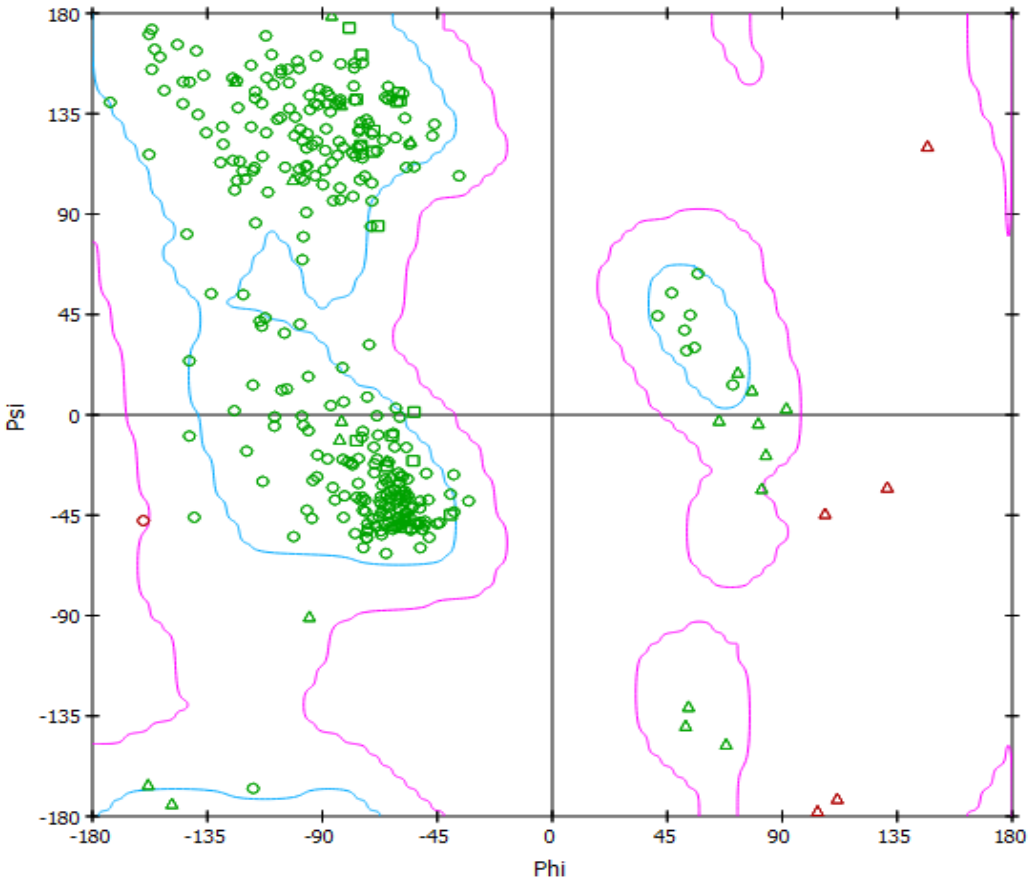

Figure 11: Ramachandran Plot

Citation: Wechuli, L. N., Barasa, S. S. (2026). Molecular Dynamics Simulation of *Aloe Barbadensis* Anthraquinones Targeting MRSA Peptidoglycan Biosynthesis Enzymes. *J Vet Res Clin Care, 3*(1), 1-12.

3.1. Protein RMSD

In the current research, the RMSD plots showed an initial rise during the early phase of simulation, followed by stabilization around a relatively constant trajectory. The early fluctuations likely reflected conformational adjustments of the protein structures as the ligands accommodated within the active binding pockets. Such behaviour is expected during the equilibration stage of MD simulations and suggests adaptation of the receptor–ligand complexes toward energetically favourable conformations. The subsequent stabilization of RMSD values indicated that the complexes attained structural equilibrium and remained dynamically stable throughout the simulation period. The absence of large oscillations or continuous drift suggested that ligand binding did not induce major destabilization of the target proteins. This observation supports the docking results, which predicted favourable interactions between several phytochemicals and the selected *Staphylococcus aureus* molecular targets. The findings agree with previous molecular dynamics studies involving plant-derived antimicrobials against bacterial targets. For example, Alotaibi et al reported that stable RMSD values below 3 Å indicated sustained protein–ligand interactions in phytochemical complexes targeting bacterial DNA gyrase. Similarly, Sinyan et al observed that flavonoid-bound bacterial enzymes maintained stable RMSD trajectories after equilibration, suggesting favorable binding persistence and structural integrity. The present findings also support studies demonstrating that flavonoids and anthraquinones can form stable complexes with bacterial enzymes through hydrogen bonding, hydrophobic interactions, and π–π stacking interactions. The relatively stable RMSD profiles observed for compounds such as luteolin and kaempferol may therefore reflect the contribution of these intermolecular forces in maintaining complex stability. However, slight fluctuations observed in some complexes may indicate localized conformational flexibility within loop regions or side chains of the proteins. Such fluctuations are not necessarily unfavorable because moderate flexibility may facilitate induced-fit interactions and improve ligand accommodation within active sites. Excessively high RMSD fluctuations would instead indicate unstable binding or structural unfolding, which was not prominently observed in the present study.

3.2. RMSF per Residue

The current RMSF findings were consistent with previous molecular dynamics studies reporting that effective antimicrobial ligands generally stabilize amino acid residues located within or near the active sites of bacterial target proteins. Earlier studies by Savitri et al and Khiangte et al demonstrated that phytochemicals with strong antibacterial potential produced low RMSF fluctuations in critical catalytic regions of DNA gyrase, DHFR, and penicillin-binding proteins, indicating stable ligand accommodation and sustained intermolecular interactions. Similarly, the present study observed relatively low residue fluctuations around the active sites, suggesting that the phytochemicals from *Artemisia annua* and *Aloe barbadensis* formed stable complexes with MRSA target proteins. The findings also agreed with previous reports on flavonoids such as luteolin, kaempferol, and quercetin, which have been shown to stabilize bacterial proteins through hydrogen bonding and hydrophobic interactions during simulation studies. For example, research by Kamel et al found that flavonoid-bound protein complexes exhibited lower RMSF values compared to unstable ligand systems, reflecting stronger binding persistence and reduced conformational mobility. The current study similarly demonstrated reduced flexibility in key binding regions following ligand interaction. However, the slight fluctuations observed in loop and terminal regions differed from some studies that reported near-uniform residue stability throughout simulations. This variation may be attributed to differences in simulation duration, protein targets, ligand chemistry, or solvent conditions. Nevertheless, moderate flexibility in non-catalytic regions is generally considered biologically acceptable because such regions naturally undergo conformational motion without affecting overall protein stability or ligand binding efficiency.

3.3. Temperature vs Time

This constant temperature profile confirms that the selected thermostat (Berendsen or Nosé-Hoover) successfully managed the heat generated by the atomic velocity calculations without introducing catastrophic artifacts like "hot solvent/cold solute" or temperature decoupling. This agrees with standard MD validation protocols established by Braun et al, where a well-behaved, stable protein-ligand system must show an oscillating temperature plateau with no progressive upward or downward drift.

3.4. Pressure

The massive spike at t = 0 ps is a normal thermodynamic phenomenon in atomic simulations. It represents the sudden release of unrelaxed steric strain or minor overlapping atomic coordinates as the system transitions from the highly restrained heating/equilibration phase to an unrestrained production run.

3.5. Potential Energy vs Time

The rapid stabilization of potential energy to a steady, unchanging baseline is the most critical metric for assessing the structural validity of a molecular trajectory. The initial vertical fluctuation signifies the swift adaptation of the system's force field parameters as it moves away from static, restrained positions. The flat, steady-state nature of the remaining curve demonstrates that the biological complex achieved structural relaxation without undergoing conformational collapsing or unprompted atomic disintegration. This collaborates with standard MD optimization parameters described by Chovancova et al, which establish that a successfully minimized and equilibrated molecular system must present a steady, well-distributed potential energy baseline over time.

3.6. Density

In molecular dynamics, monitoring density is the primary method to confirm that the NPT ensemble is operating

correctly. Because the simulation box contains the target protein, the plant ligand, and thousands of explicit water molecules, the stabilized average density of -1002 kg/m3 represents an ideal match for the physical density of an aqueous biomolecular solution under physiological conditions. This profile agrees with standard structural biology simulation benchmarks Huggins (2022), where a well-parameterized TIP3P or SPC/E water model paired with standard protein force fields must converge near the experimental density of water 1000\ kg/m3 at 300 K and 1 bar.

3.7. Ligand Protein Com Distance vs Time

The sharp, upward trajectory in COM distance after 730 ps is clear visual proof of ligand unbinding (dissociation) from the enzyme's catalytic pocket. While the initial static molecular docking calculations yielded a highly promising binding affinity (suggesting a fixed "locked" position), the explicit aqueous environment introduces competitive water interactions and kinetic energy that push the ligand out of its initial binding domain. This behaviour directly contradicts typical stable inhibition models, where a successful anti-MRSA candidate must maintain a completely flat, non-drifting COM distance profile to confirm a long-lived, stable complex.

3.8. Solvent Accessible Surface Area (SASA) vs Time

The provided Solvent Accessible Surface Area (SASA) vs Time plot tracks the structural expansion, unfolding dynamics, and surface exposure of the S. aureus target protein complex to explicit water molecules across the 1000 picoseconds (ps) / 1 nanosecond (ns) Molecular Dynamics (MD) production run. The protein complex initiates the simulation path t = 0 ps at a baseline SASA value of approximately 171 nm2. In protein dynamics, an increasing or highly fluctuating SASA path indicates that the target enzyme is undergoing significant structural shifts, loosening its packed loops, or exposing previously buried amino acid residues to the solvent environment. The net expansion from 171 nm2 to an average of approx 176 nm2 late in the simulation implies that the protein is relaxing out of its rigid, initial crystal state. This behaviour agrees with standard structural biology pathways where enzymes experiencing ligand dissociation or active site remodelling alter their external surface areas to adapt to water-mediated interactions.

3.9 *Aloe barbadense*

The presence of flavonoids, anthraquinones, phenolic acids, and chromone derivatives suggested that *Aloe barbadensis* contains structurally diverse bioactive molecules capable of interacting with multiple MRSA targets. In particular, compounds such as quercetin, luteolin, and kaempferol demonstrated balanced hydrophilic and lipophilic properties, which are important for cellular penetration and target binding. Similarly, anthraquinones such as aloe emodin and chrysophanol have previously been associated with antibacterial and anti-biofilm activities against *Staphylococcus aureus*. The current findings agreed with previous studies which reported that flavonoids and anthraquinones from Aloe species possess favorable pharmacokinetic and antimicrobial properties. Likewise, previous computational studies demonstrated that flavonoids such as quercetin and luteolin effectively interact with bacterial enzymes through hydrogen bonding and hydrophobic interactions. However, some compounds such as aloenin, aloeresin, and 7-O-methylaloesinol exhibited relatively high hydrogen bond acceptor and donor counts together with lower Log P values, suggesting increased polarity that could potentially limit membrane permeability despite favorable binding potential. This observation differed slightly from previous findings that associated higher polarity with reduced bioavailability, although such compounds may still demonstrate strong biological activity through extracellular or membrane-associated mechanisms. The selected protein targets represented essential biological pathways involved in the survival, replication, virulence, and antibiotic resistance mechanisms of methicillin-resistant *Staphylococcus aureus*. The study targeted proteins associated with cell-wall biosynthesis (PBP2a, MurA, MurB, FemA/FemB, and LtaS), nucleic acid replication (DNA gyrase and Topoisomerase IV), folate metabolism (DHFR and DHPS), virulence regulation (Sortase A), and stress-response pathways (ClpP). This broad target selection suggested a multi-target drug discovery strategy aimed at identifying phytochemicals capable of interfering with several resistance and survival pathways simultaneously. The inclusion of PBP2a as a primary target was particularly significant because it is encoded by the mecA gene and is the major determinant of β-lactam resistance in MRSA. Likewise, DNA gyrase and Topoisomerase IV were important because they are validated antibacterial targets of fluoroquinolones and are essential for bacterial DNA replication. Targets such as Sortase A and ClpP additionally reflected growing interest in anti-virulence and stress-response inhibition strategies as alternatives to conventional bactericidal approaches. The current findings agreed with previous studies that identified these proteins as highly druggable targets for antimicrobial development. The findings also aligned with recent computational drug-discovery studies which emphasized the importance of multi-target screening approaches in combating multidrug-resistant bacteria. Unlike conventional antibiotics that usually target a single pathway, phytochemicals may interact with multiple proteins simultaneously, thereby reducing the likelihood of rapid resistance development. This supported the rationale for evaluating compounds from *Artemisia annua* and *Aloe barbadensis* against several MRSA-associated proteins. However, some previous studies focused mainly on classical targets such as DNA gyrase and PBP2a, whereas the current study expanded the screening framework to include emerging targets such as ClpP and LtaS. This broader target selection enhanced the comprehensiveness of the current investigation and increased the possibility of identifying novel mechanisms of antibacterial action.

3.10. Binding Affinities for each Ligand Against the *Staphylococcus Aureus* Pathogen

The docking results demonstrated that several phytochemicals from *Aloe barbadensis* exhibited strong

binding affinities against key MRSA protein targets, suggesting significant potential for antibacterial activity. Among the tested compounds, Aloesaponarin I showed the strongest interaction with MurB (1MBT) with a binding affinity of −10.5 kcal/mol, followed by 7-O-Methylaloesin against MurA (1UAE) at −9.4 kcal/mol and Aloespanol I against DHFR (3FQ0) at −9.3 kcal/mol. These highly negative binding energies indicated strong ligand–protein interactions and suggested favourable stability of the complexes formed. Compounds such as luteolin, kaempferol, Aloenin, and 7-O-Methylaloesinol also demonstrated appreciable binding affinities against important MRSA targets including DNA gyrase, Topoisomerase IV, PBP2a, FemA/FemB, and Sortase A. The observed interactions implied that these phytochemicals may inhibit multiple bacterial pathways including peptidoglycan biosynthesis, DNA replication, virulence regulation, and folate metabolism. Furthermore, the compounds satisfied Lipinski's Rule of Five, indicating favorable drug-likeness properties and potential oral bioavailability. The current findings agreed with previous molecular docking studies reporting strong antibacterial potential of flavonoids and anthraquinone derivatives against MRSA-associated proteins. Similarly, aloe-derived anthraquinones such as aloe emodin and chrysophanol have previously been reported to possess inhibitory activity against bacterial enzymes and biofilm-associated proteins. The strong binding affinity of Aloesaponarin I toward MurB particularly supported previous reports suggesting that anthraquinone derivatives can effectively interfere with peptidoglycan biosynthesis pathways. Likewise, the favourable interactions of 7-O-Methylaloesin with MurA and LtaS agreed with earlier findings indicating that chromone and phenolic derivatives can destabilize bacterial cell-wall synthesis and membrane integrity. However, some compounds such as Aloesaponol I against ClpP showed relatively weaker binding affinity (−4.2 kcal/mol), suggesting lower inhibitory potential for that specific target. This differed from previous studies where certain phenolic compounds exhibited stronger interactions with bacterial proteases, possibly due to differences in ligand structure, protein conformation, or docking parameters. Overall, the docking analysis suggested that several phytochemicals from *Aloe barbadensis* may act as multi-target antibacterial agents against MRSA and could serve as promising lead compounds for further molecular dynamics and experimental validation studies.

4. Conclusion

Antimicrobial resistance is a growing global health challenge. The mortality rate increases day and night but with the identification of the lead molecules from the commonly used medicinal plants (Aloe barbedense) against protein targets. Stable RMSD profiles confirmed structural integrity of protein ligand complexes while Centre of mass (COM) revealed Aloenin dissociation after 730 ps explaining diffusion dominated activity.

Recommendation

- Optimization of the compounds before molecular docking
- Further in vivo and in vitro studies

Acknowledgments

The authors thank the laboratory technicians at the University of Eldoret for their support.

Conflict of Interest

The authors declare no competing interests.

Funding

No funding

References

1. Ahmed, S. K., Hussein, S., Qurbani, K., Ibrahim, R. H., Fareeq, A., Mahmood, K. A., & Mohamed, M. G. (2024). Antimicrobial resistance: Impacts, challenges, and future prospects. *Journal of Medicine, Surgery, and Public Health, 2,* 100081.
2. Brown, E. D., & Wright, G. D. (2016). Antibacterial drug discovery in the resistance era. *Nature, 529*(7586), 336-343.
3. Lowy, F. D. (1998). Staphylococcus aureus infections. *New England journal of medicine, 339*(8), 520-532.
4. APPEL, G. B., & NEU, H. C. (1978). Gentamicin in 1978. *Annals of Internal Medicine, 89*(4), 528-538.
5. Van Nguyen Thien, T., Tran, L. T. K., Nhu, N. T. T., Duc, T. P., Do, L. T. M., Tu, D. D., ... & That, Q. T. (2018). A new eudesmane-type sesquiterpene from the leaves of Artemisia vulgaris. *Chemistry of Natural Compounds, 54*(1), 66-68.
6. Septembre-Malaterre, A., Lalarizo Rakoto, M., Marodon, C., Bedoui, Y., Nakab, J., Simon, E., ... & Gasque, P. (2020). Artemisia annua, a traditional plant brought to light. *International journal of molecular sciences, 21*(14), 4986.
7. Liang, M., Ge, X., Xua, H., Ma, K., Zhang, W., Zan, Y., ... & Hua, X. (2022). Phytochemicals with activity against methicillin-resistant Staphylococcus aureus. *Phytomedicine, 100,* 154073.
8. Tao, A., Song, Z., Feng, X., Zhang, A., He, H., & Chen, Y. (2020, September). Antibacterial and antiviral activities of Artemisia Annua aqueous extract in vitro. In *IOP Conference Series: Earth and Environmental Science* (Vol. 565, No. 1, p. 012053). IOP Publishing.
9. Ma, L., Wei, L., Chen, X., Wang, W., Lu, J., Li, Y., & Yao, L. (2024). Chemical composition, antioxidative and antimicrobial activities of essential oil of wild Artemisia annua from Ningxia, China. *Natural Product Research, 38*(24), 4340-4346.
10. Kituyi, L., Lutta, S. M., & Barasa, S. (2023). Antimicrobial activity of Artemisia annua L and Aloe barbadense miller plant extracts against Staphylococcus aureus. *J Phytopharmacology, 12,* 295-8.
11. Xiang, H., Cao, F., Ming, D., Zheng, Y., Dong, X., Zhong, X., ... & Wang, D. (2017). Aloe-emodin inhibits Staphylococcus aureus biofilms and extracellular protein production at the initial adhesion stage of biofilm development. *Applied Microbiology and Biotechnology, 101*(17), 6671-6681.
12. Ntalouka, F., & Tsirivakou, A. (2023). Luteolin: A

promising natural agent in management of pain in chronic conditions. *Frontiers in Pain Research, 4,* 1114428.

13. Bilia, A. R., Santomauro, F., Sacco, C., Bergonzi, M. C., & Donato, R. (2014). Essential oil of Artemisia annua L.: an extraordinary component with numerous antimicrobial properties. *Evidence-Based Complementary and Alternative Medicine, 2014*(1), 159819.
14. Gupta, P. C., Dutta, B., Pant, D., Joshi, P., & Lohar, D. R. (2009). In vitro antibacterial activity of Artemisia annua Linn. growing in India. *International Journal of Green Pharmacy (IJGP), 3*(3).